DOI: 10.1002/ejic.200601096

Mutual Influence of Spacer Length and Noncoordinating Anions on Thermal and Light-Induced Spin-Crossover Properties of Iron(II)–α,ω-Bis(tetrazol-1-yl)-alkane Coordination Polymers

Alina Absmeier,[a,b] Matthias Bartel,[a,c] Chiara Carbonera,[b] Guy N. L. Jameson,[d] Franz Werner,[a] Michael Reissner,[e] Andrea Caneschi,[c] Jean-François Létard,[b] and Wolfgang Linert*[a]

Keywords: Iron(II) / Magnetic properties / Coordination polymers / Photomagnetism / Spin crossover

The influence of noncoordinating anions is analysed in an extension of our systematic investigations into iron(II) spin-crossover coordination polymers. We present here ditetrazole complexes of iron(II) tetrafluoroborate where the two tetrazole moieties are separated by alkylene spacers. The number of carbon atoms in the spacer (*n*) was varied between *n* = 5–10, 12, and the complexes were compared with their ClO_4^- analogues. Pronounced magnetic and magneto-optical differences were found in the comparison of the two series. A chain-type arrangement in the complexes' crystal structures is proposed with decreased interactions between iron centres as *n* increases, leading to more gradual spin transitions. When *n* = 5–7 the smaller tetrafluoroborate causes the spin transitions of the respective complexes to occur at higher temperatures than those of the equivalent perchlorate series. Both series exhibit a parity effect, but at *n* = 8 the parity effect reverses for tetrafluoroborate. With increasing *n*, however, iron–iron interactions seem to fade away and a limiting value of T_{SC} = 160 K is approached by both series.

Introduction

Interest in multifunctional spin-crossover (SC) compounds within more complicated structural frameworks has increased dramatically in recent years,[1–3] leading to the discovery of exciting magnetic and photomagnetic properties. These investigations have yielded 1D,[4–8] 2D[9] and 3D[10–15] coordination polymers using iron(II) as the SC species. Our group has focused its recent research efforts on ditetrazole ligands with varying length alkylene spacer groups between the coordinating tetrazole groups, hereafter referred to as *n*ditz (see Figure 1). Within this family, short spacers (two carbon atoms) lead to 1D chain networks,[4] whilst four carbon atoms lead to 3D networks.[16,17] To build these frameworks not only is the number of carbon atoms (*n*) in the bridging alkylene groups in the ditetrazole ligand important, but the noncoordinating anion is also important. Anions are also believed to influence the SC behaviour of coordination compounds, varying spin transition temperatures and cooperative effects associated with the sharpness and hysteresis of the transition.[7,18–22]

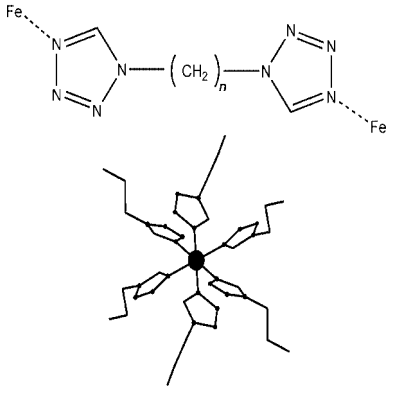

Figure 1. The ditetrazole ligand used and the octahedral geometry around iron(II).

In a previous investigation[23] we reported detailed magneto-optical data for a series (*n* = 4–9) using perchlorate as the anion, which showed an interesting dependence between the magneto-optical properties and the parity of the alky-

[a] Institute of Applied Synthetic Chemistry, Vienna University of Technology,
Getreidemarkt 9/163-AC, 1060 Vienna, Austria
Fax: +43-1-58801-16299
E-mail: wlinert@mail.zserv.tuwien.ac.at
[b] Institut de Chimie de la Matière Condensée de Bordeaux, UPR CNRS No 9048, Université Bordeaux 1, Groupe des Sciences Moléculaires,
87 Av. du Doc. A. Schweitzer, 33608 Pessac, France
[c] LAMM, Dipartimento di Chimica & UdR INSTM, Università di Firenze,
Via della Lastruccia 3, 50019 Sesto F.no, Italy
[d] Department of Chemistry, University of Otago,
P. O. Box 56, Dunedin, New Zealand
[e] Institute for Solid State Physics, Vienna University of Technology,
Wiedner Hauptstraße 8–10/138, 1040 Vienna, Austria

lene spacer. In order to compare and contrast the results obtained for the perchlorates,[23] we synthesised an analogous series (n = 5–9) of complexes with the tetrafluoroborate anion and extended both series up to n = 12. Tetrafluoroborate is known to be of similar size, geometry and chemical hardness to perchlorate. Indeed, the estimated ionic radii are 2.29 Å for BF_4^- and 2.37 Å for ClO_4^-.[24] Furthermore, the polymers were identically prepared and this minimised differences. We did not want to change the structure of the complexes considerably by using bigger, softer and geometrically different anions such as PF_6^- or SbF_6^- because then a direct comparison would be unsound. We present here a comparison of the magneto-optical properties and provide tentative structural information based on comparative X-ray powder diffraction (XRPD) studies of the two series. As seen from preliminary inspections of X-ray patterns, $[Fe(4ditz)_3](BF_4)_2$ and $[Fe(4ditz)_3](ClO_4)_2$ adopt completely different structures when compared with the complexes with longer spacers and are therefore excluded from this report and will be presented in a separate paper. Taking into consideration the small decrease in diameter in going from ClO_4^- to BF_4^-, the difference in properties are far greater than anticipated.

Results and Discussion

Powder Diffraction

As it was impossible to grow single crystals of the title materials, the microcrystalline samples were investigated by XRPD. The homologous series $[Fe(n\text{ditz})_3](X)_2\cdot EtOH$ (n = 5–10, 12; X = BF_4^-, ClO_4^-) are characterised as follows (Figure 2): (i) The perchlorate compounds[23] show a higher degree of crystallinity compared with that of the tetrafluoroborates. (ii) The diffractograms are very similar in shape. (iii) The reflection with the longest d-spacing is the strongest and is shifted systematically to lower diffraction angles with increasing alkyl chain length. (iv) The reflections broaden with increasing n and level off to background at $2\theta \approx 35°$, while the half-widths of the longest ones are more or less conserved. (v) All phases form very thin platelike microcrystallites with a thickness of a fraction of a micrometer.

Point (ii) lets us conclude that the phases exhibit more or less the same basic structure. The reflection broadening can be explained by size effects due to the extremely thin plates. As the largest crystallographic axis is usually the direction of the lowest crystal growth rate, the base plane of the microplates lies perpendicular to the longest cell axis. The reflection with the largest d-spacing, showing a steady shift as n increases, can be regarded as this axis (possibly of higher order) that mirrors the increasing number of methylene groups in the ligands. Powder indexing of the phase $[Fe(5ditz)_3](BF_4)_2\cdot EtOH$, with the positions of the first 20 reflections determined using the DICVOL program,[25] yielded a preliminary solution in the monoclinic crystal system (pseudohexagonal): a = 10.99, b = 20.37, c = 10.07 Å, $\alpha = \gamma = 90$, β = 126.1°, V = 1822 Å^3, M_{20} = 13, which is in

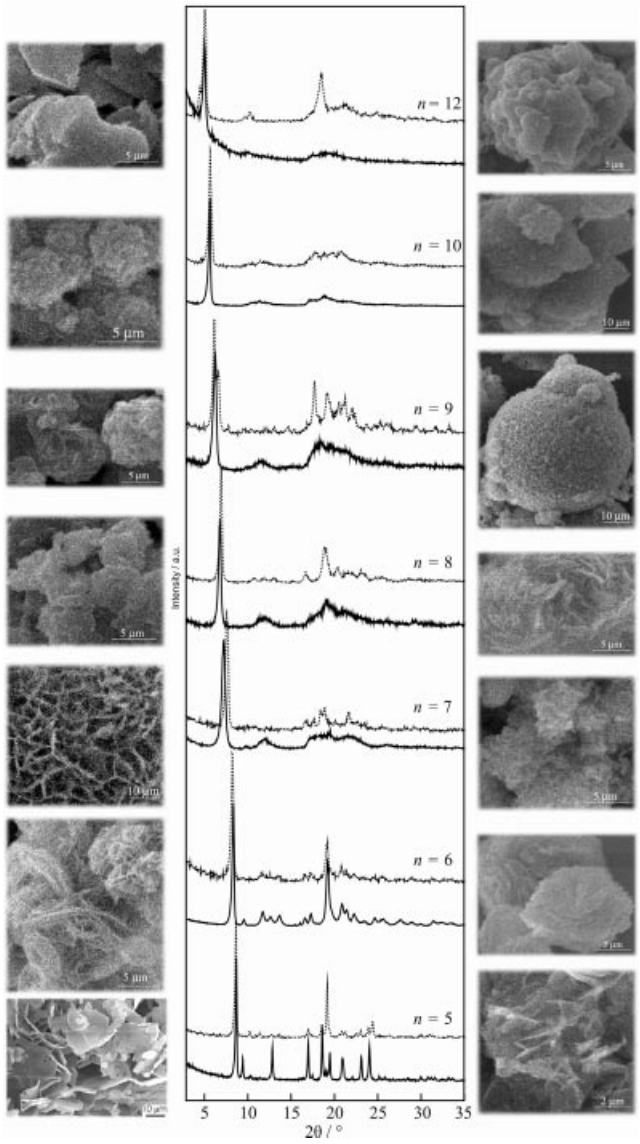

Figure 2. Comparison of the $[Fe(n\text{ditz})_3](BF_4)_2\cdot EtOH$ (n = 5–10, 12; solid) series' X-ray powder patterns (λ = Cu-$K_{\alpha 1,2}$) with those of the corresponding perchlorates (upper lines), flanked by the corresponding SEM images (BF_4^- left, ClO_4^- right).

accordance with a unit cell content of Z = 2. This metric can be regarded as a distorted variant of the trigonal symmetry found for $[Fe(2ditz)_3](BF_4)_2$[4] with comparable lattice parameters: $a = b$ = 10.380(1), c = 14.953(3) Å, V = 1395.3(3) Å^3 [at 296(2) K, the shortened c axis is caused by the ethylene spacer]. Therefore we tend to describe the pentylene- to dodecylene-ditetrazole complex series in a chain-type arrangement as well. The higher order complexes are suspected to crystallise in the triclinic system which, however, is not possible to confirm from the low-quality powder patterns. Calculating the unit cell volumes for the phases under investigation, assuming the monoclinic cell from earlier and setting the b axis length to $d\times 2$ of the longest line (i.e., the 020 reflection), results in unit cell contents Z ca. 2, which again is in accordance with the $[Fe(2ditz)_3](BF_4)_2$ complex. In Figure 3 an idealised tenta-

tive structural proposition is depicted. The ligands, linked together by iron(II), are stretched out and aligned parallel in a hexagonal close-packed manner with the counterions in between the chains. Increases in the alkylene spacer length will expand the unit cell in the crystallographic direction of the chains, leaving the other two untouched. Additionally, the voids between them become larger and are likely to be filled with presumably disordered and nonstoichiometric amounts of solvent molecules. As the interaction between the chains is weak [the Coulomb forces between the positively charged iron(II) and BF_4^- will diminish with increasing *n*], stacking faults are favoured by longer spacers, and additional reflection broadening is likely to be observed.

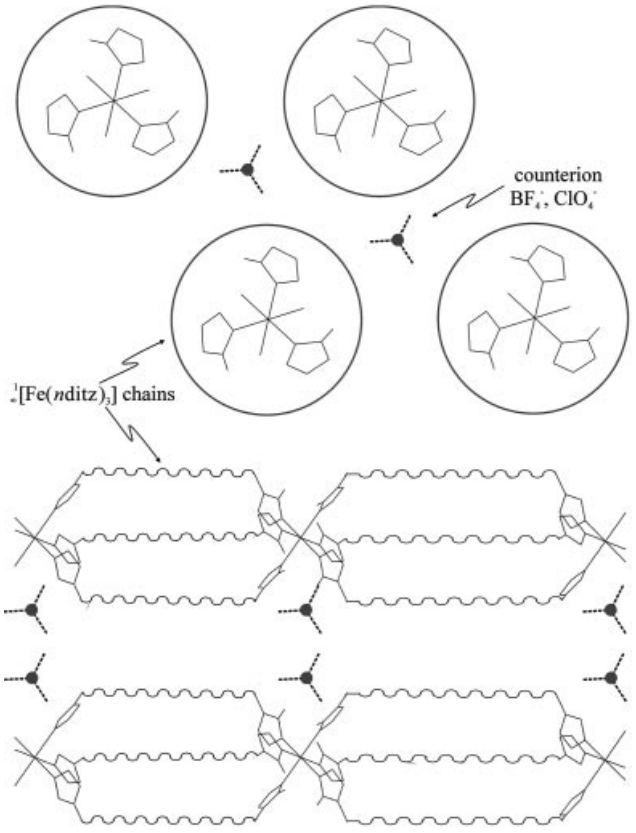

Figure 3. Tentative basic structural model of the $[Fe(nditz)_3](X)_2 \cdot EtOH$ (n = 5–10, 12; X = BF_4^-, ClO_4^-) phases viewed along the $[Fe(nditz)_3]^{2+}$ chains (circled, top) and the perpendicular direction (bottom). The orientation and geometry of the complex is presumed arbitrarily.

Optical Properties

As expected, all members of the series show a thermochromic effect associated with a spin transition, that is, from white in the HS state at room temperature to violet in the LS state at lower temperatures. The result of a typical temperature-dependent reflectivity experiment, which is a preliminary test for the LIESST (light-induced excited spin-state trapping) measurement (see below), is illustrated in Figure 4, using $[Fe(5ditz)_3](BF_4)_2$ as an example. No significant differences are found between the BF_4^- and ClO_4^- series. The spectra shown are measured within the range 450–900 nm at particular temperatures between 10 and 290 K and clearly show the presence of the expected d-d transitions of an octahedrally coordinated Fe^{II} complex: the $^5T_2 \rightarrow {}^5E$ band at 830 nm when HS and the $^1A_1 \rightarrow {}^1T_1$ band at 570 nm when LS. The second LS transition, $^1A_1 \rightarrow {}^1T_2$, normally observable at 370 nm, is not within the range of the instrument. In addition, we recorded the change in intensity of both HS and LS bands as a function of temperature under constant light irradiation (see inset in Figure 4) by following changes in the reflectivity occurring at (830 ± 2.5) and (550 ± 2.5) nm.

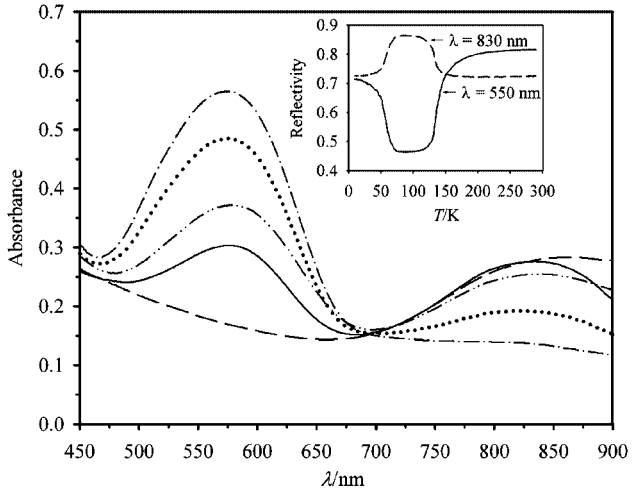

Figure 4. Reflectivity measurements of $[Fe(5ditz)_3](BF_4)_2$ as a function of temperature. Absorbance spectra at 280 K (– –), 140 K (– · · –), 80 K (– · –), 60 K (···) and 10 K (–) are shown. The inset reports the reflectivity followed at (550 ± 2.5) and (830 ± 2.5) nm.

For all compounds, at room temperature only the HS band is visible, whilst at 80 K only the LS transition is observable. Below 80 K, however, the reflectivity experiment demonstrates the existence of a photoinduced phenomenon at the surface. In fact, at low temperatures the sample was seen to bleach (see Figure 4 and inset), indicating the occurrence of a LS/HS photoconversion through the LIESST effect. For each compound, we calculated the amount of photobleached fraction (%Irr-Surface; reported in Table 1) relative to the value found at room temperature. However, similar to the previously published ClO_4^- analogues,[23] the higher the T_{SC}, the lower the level of the light-induced LS/HS transformation as described by the inverse energy-gap law by Hauser[26] and the $T(LIESST)/T_{SC}$ relation introduced by Letard.[27] Magneto-optical parameters of $[Fe(nditz)_3](X)_2$ where n = 10, 12 and X = BF_4^-, ClO_4^- were not measured.

Table 1. Spin transition, reflectivity and LIESST parameters of the discussed complexes.

	X = BF_4^-				X = ClO_4^-[a]			
$[Fe(n\text{ditz})_3](X)_2$	T_{SC}/K	T(LIESST)/K	%Irr-Surface[b]	%Irr-Bulk[c]	T_{SC}/K[d]	T(LIESST)/K	%Irr-Surface[b]	%Irr-Bulk[c]
5	131	58	71	84	125	52	64	72
6	164	_[e]	34	25	155	_[e]	42	43
7	154	58	47	71	144	51	42	57
8	148	52	47	55	169	_[e]	14	13
9	154	50[f]	50	36	155	37	26	47
10[g]	150	–	–	–	160	–	–	–
12[g]	156	–	–	–	159	–	–	–

[a] Data taken from ref.[23] [b] Percentage of the sample photobleached. [c] Percentage conversion to the metastable high spin state by irradiation at 10 K. [d] T_{SC} is the temperature of the spin transition estimated from the maximum in the first derivative of the $\chi_M T$ vs. T plot. [e] No minimum in $d(\chi_M T)/d(T)$ observable. [f] No minimum in $d(\chi_M T)/d(T)$ observable: estimated from the obtained relaxation curve of the LIESST experiment. [g] No magneto-optical data available.

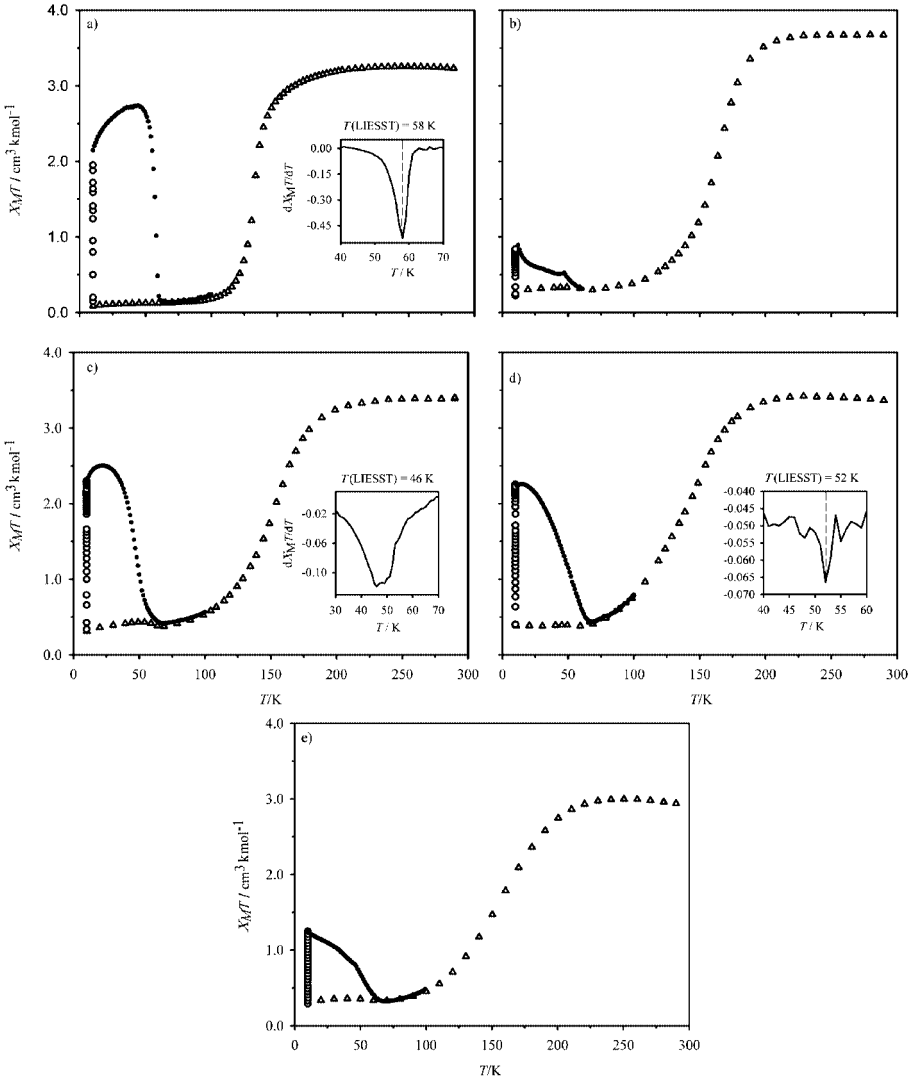

Figure 5. Temperature dependence of $\chi_M T$ for (a) $[Fe(5ditz)_3](BF_4)_2$, (b) $[Fe(6ditz)_3](BF_4)_2$, (c) $[Fe(7ditz)_3](BF_4)_2$, (d) $[Fe(8ditz)_3](BF_4)_2$, (e) $[Fe(9ditz)_3](BF_4)_2$. (Δ) Data recorded without irradiation; (○) data recorded during irradiation at 10 K; (●) T(LIESST) measurement, data recorded in the warming mode with the laser turned off after irradiation for one hour. The existence of a small anomaly at around 50 K on the T(LIESST) curve corresponds to a remnant oxygen contamination even if particular precaution was taken to purge the SQUID cavity for one hour at room temperature.

Magnetic and Photomagnetic Properties

Susceptibility curves were measured between 10 and 300 K for all compounds, and the obtained curves depicting $\chi_M T$ versus T, where χ_M is the molar magnetic susceptibility and T is the temperature, are shown in Figure 5. The temperature of the thermal spin transition, T_{SC}, estimated from the maximum in the first derivative of the $\chi_M T$ versus T plot, is given in Table 1. Photomagnetic measurements were carried out as previously published,[23] and this procedure allowed the quantification of T(LIESST) (see Table 1), which is determined by the minimum of the $d(\chi_M T)/d(T)$ versus T curve recorded during thermal-induced relaxation.[28] Figure 5 shows the photomagnetic behaviour, and Table 1 shows for each compound the percentage of photoconversion obtained by irradiation at 10 K relative to the magnetic value recorded at room temperature where a pure HS state is assumed (%Irr-Bulk).

All compounds {$[Fe(n\text{ditz})_3](X)_2$, n = 5–10, 12; X = BF_4^-, ClO_4^-} undergo a complete spin transition between 100 and 220 K (see Figure 5, a–e) and reach a $\chi_M T$ product close to 3.3 $cm^3 \cdot K \cdot mol^{-1}$, in agreement with the theoretically expected value for HS Fe^{II} compounds at room temperature.

At low temperatures in some of the curves, a residual magnetisation is observed yielding a $\chi_M T$ value up to 0.4 $cm^3 \cdot K \cdot mol^{-1}$, which might be caused by thermally inactive HS iron(II) or traces of iron(III). Comparison of the new magnetic data with the perchlorate data shows a similar trend for n = 5–7. The SC curves themselves are all very similar with the $[Fe(5ditz)_3](BF_4)_2$ transition curve a little steeper. The temperatures of transition, T_{SC}, are all higher for BF_4^- than for ClO_4^-. The %Irr-Surface and %Irr-Bulk values show a similar relationship with n but the actual values are different, suggesting a similar relationship with parity. There is, however, a variation when n is changed from 7 to 8. Here T_{SC} of $[Fe(8ditz)_3](BF_4)_2$ is lower and the transition itself is a lot more gradual than its perchlorate analogue, while %Irr-Surface and %Irr-Bulk are significantly higher. This reversal of the parity dependence at this point suggests that the smaller BF_4^- causes a change in the arrangement of the alkyl chains. By n = 9, the transition is very gradual and almost exactly the same in both cases (T_{SC} = 154 K for BF_4^- and 155 K for ClO_4^-). The lowered $\chi_M T$ value at high temperature for the BF_4^- complex is caused by LS Fe^{II} or LS Fe^{III} impurities. $[Fe(10ditz)_3](ClO_4)_2$ has a flatter magnetic curve than that of the BF_4^- analogue but T_{SC} is 10 K higher (see Figure 6). However by n = 12, the transitions are remarkably similar again (see Figure 6). This might be because any further changes in the arrangement of the alkyl chains would now be insignificant with respect to the greater separation of the iron centres.

The larger iron–iron distances and disorder should lead to a concomitant decrease in cooperativity between iron centres until the transition can be described by a simple Boltzmann distribution. This behaviour is supported by the magnetic properties around the transition temperature. The slope at the inflection point of the transition curves (T_{SC}) is plotted in Figure 7. It can be seen that the spin transition curves become more gradual with increasing n as expected. This lends further support to the suggestion that all compounds in the series produce a chain-type arrangement, as proposed in the XRPD section.

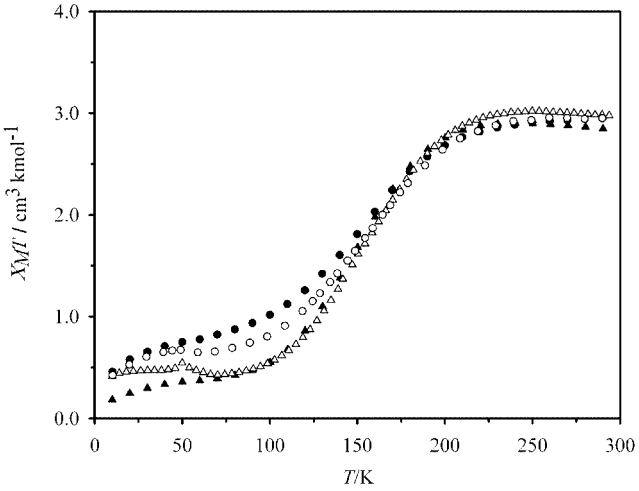

Figure 6. Temperature dependence of $\chi_M T$ for (a) $[Fe(10ditz)_3](BF_4)_2$ (▲) and $[Fe(10ditz)_3](ClO_4)_2$ (●) and b) $[Fe(12ditz)_3](BF_4)_2$ (Δ) and $[Fe(12ditz)_3](ClO_4)_2$ (○), in the heating mode. The existence of a small anomaly at around 50 K on the curves almost certainly corresponds to a remnant oxygen contamination.

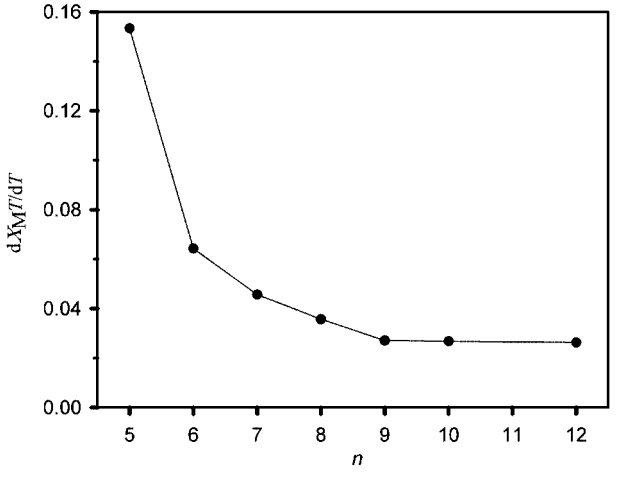

Figure 7. The slope of the $\chi_M T$ curves of the BF_4^- series at the transition temperature (T_{SC}) for n = 5–10, 12, in the heating mode. The line connecting the points has no physical meaning and is intended only as a guide.

Conclusions

We present here a detailed study of a homologous series of iron(II) SC coordination polymers using BF_4^- as the counteranion and compare this data with our previous study of closely related compounds[23] using the same ligands but with ClO_4^- as the counteranion. By changing the anion to BF_4^-, we observed that the structure has changed slightly and thus altered the SC behaviour. As indicated by XRPD, the phases seem to adopt a 1D polymer by forming

chains, arranged approximately in a hexagonal close-packed manner. The longer the alkylene spacer, the higher the disorder of the infinite 1D network as indicated by severe reflection broadening.

In Figure 8, T_{SC} versus n is shown for the BF_4^- and the ClO_4^- series. Both curves show a zigzag behaviour with decreasing amplitude, reaching a similar end point. Indeed, $[Fe(12ditz)_3](ClO_4)_2$ has a T_{SC} = 159 K and $[Fe(12ditz)_3](BF_4)_2$ has a T_{SC} = 156 K. This suggests that as the alkylene spacer is lengthened, T_{SC} eventually reaches a limiting value of 160 K. It is, however, obvious that the tetrafluoroborates show a reversal in the parity effect as n is increased from 7 to 8. This suggests that at this length the alkylene chains are differently arranged. In contrast, the perchlorates show a parity effect up to n = 12[23] (see Figure 8).

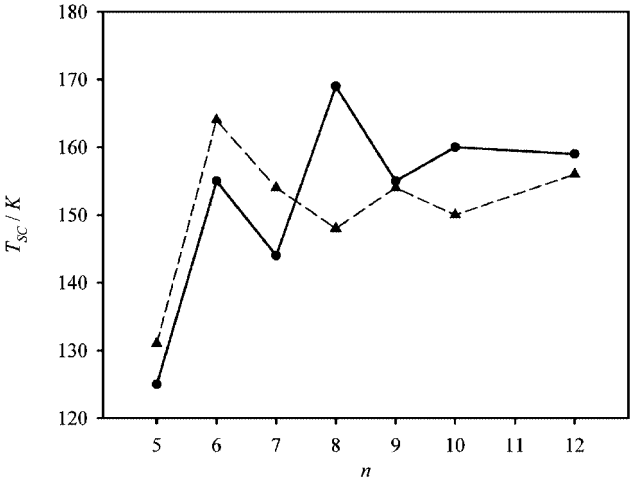

Figure 8. Comparison of T_{SC} as a function of the number of carbon atoms (n) in the spacer of the ditetrazole ligands for the BF_4^- (▲) and ClO_4^- (●) series.

Chemical intuition would suggest more or less identical results for such similar noncoordinating anions like perchlorate and tetrafluoroborate. In spite of this, our investigations on these two related series clearly show that there is a anion dependence, especially in terms of their magneto-optical behaviour. Furthermore, the pronounced dependence of T_{SC} upon the parity of the spacer length which was found in the perchlorate series is also found, with alterations, in the tetrafluoroborate over the whole series (see Figure 8). Eventually, however, both series reach the same limiting value of T_{SC} at high n when orientation is insignificant with respect to the separation of the iron centres. As far as we can derive from our studies, the choice of the ligand system represents the fundamental requirement to obtain a SC compound, but the impact of the noncoordinating anion seems to be of similar importance. With this in mind, the interest is now focused on complexes in which the interaction of anion and ligand leads to optimised systems where the spin transition and cooperativity can be systematically tuned to be used for future applications of new materials with interesting magneto-optical features.

Experimental Section

Chemicals and Standard Physical Characterisation: Iron(II) tetrafluoroborate hexahydrate was obtained from Aldrich. All other chemicals were standard reagent grade and used as supplied. Elemental analyses (C, H and N) were performed in the laboratories of Dr. Roman Boca (Slovenská Vyská Scola Technicá v Bratislava, Chemitechothenologická Fakulta, Radlinského 9, 81237 Bratislava, Slovakia). Mid-range FTIR spectra of the compounds were recorded as KBr pellets within the range of 4400–450 cm^{-1} using a Perkin–Elmer 16PC FTIR spectrometer. Pellets were obtained by pressing the powdered mixture of the samples in KBr in vacuo using a hydraulic press applying a pressure of 10000 $kg \cdot cm^{-2}$ for 5 min.

Synthesis of the Complexes: The general synthetic pathway and the synthesis of the ligands used [1,*n*-bis(tetrazol-1-yl)alkane; n = 5–10, 12] has been previously reported.[17,23,29,30] Note that the 1,11-bis(tetrazol-1-yl)undecan has not yet been synthesised. The respective ligand (*n*ditz, 1 mmol) was dissolved in reagent grade ethanol (n = 5–10, 12). While the solution cooled down to 40 °C, iron(II) tetrafluoroborate hexahydrate or iron(II) perchlorate hexahydrate (0.33 mmol) and a small amount of ascorbic acid to keep the iron as iron(II) were diluted in ethanol (5 mL). This solution was slowly added to the dissolved ligand, and the resulting mixture was stirred for 4 h. The precipitate was filtered off, and the obtained powder was dried with P_2O_5. It has so far proved impossible to grow single crystals by any of the standard methods including H-tube slow diffusion or slow cooling.

Elemental Analyses and Mid-FTIR

$[Fe(5ditz)_3](BF_4)_2$: Yield: 0.16 g (59%). $C_{21}H_{36}B_2F_8FeN_{24}$ (854.14): calcd. C 29.53, H 4.25, N 39.36; found C 29.30, H 4.18, N 37.66. Mid-FTIR: $\tilde{\nu}$ = 3146 (C–H stretching vibration, ν, of the aromatic tetrazole ring), 2949, 2933 and 2862 (ν_{C-H} of the aliphatic C–H in the butylene spacer), 1506, 1370 ($\nu_{N=N}$, ν_{C-N}), 1183, 1109 ($\nu_{C=N}$, ν_{N-N}, ν_{C-N}) cm^{-1}.

$[Fe(6ditz)_3](BF_4)_2$: Yield: 0.15 g (50%). $C_{24}H_{42}B_2F_8FeN_{24}$ (896.22): calcd. C 32.16, H 4.72, N 37.51; found C 31.41, H 4.78, N 36.15. Mid-FTIR: $\tilde{\nu}$ = 3148 (ν_{C-H} of the aromatic tetrazole ring), 2938 and 2862 (ν_{C-H} of the aliphatic C–H in the butylene spacer), 1506, 1372 ($\nu_{N=N}$, ν_{C-N}), 1182, 1102 ($\nu_{C=N}$, ν_{N-N}, ν_{C-N}) cm^{-1}.

$[Fe(7ditz)_3](BF_4)_2$: Yield: 0.19 g (61%). $C_{27}H_{48}B_2F_8FeN_{24}$ (938.31): calcd. C 34.56, H 5.16, N 35.83; found C 34.00, H 5.18, N 35.72. Mid-FTIR: $\tilde{\nu}$ = 3147 (ν_{C-H} of the aromatic tetrazole ring), 2940 and 2862 (ν_{C-H} of the aliphatic C–H in the butylene spacer), 1507, 1375 ($\nu_{N=N}$, ν_{C-N}), 1173, 1108 ($\nu_{C=N}$, ν_{N-N}, ν_{C-N}) cm^{-1}.

$[Fe(8ditz)_3](BF_4)_2$: Yield: 0.18 g (55%). $C_{30}H_{54}B_2F_8FeN_{24}$ (980.39): calcd. C 36.75, H 5.55, N 34.29; found C 36.84, H 5.58, N 33.63. Mid-FTIR: $\tilde{\nu}$ = 3148 (ν_{C-H} of the aromatic tetrazole ring), 2936 and 2859 (ν_{C-H} of the aliphatic C–H in the butylene spacer), 1507, 1368 ($\nu_{N=N}$, ν_{C-N}), 1183, 1102 ($\nu_{C=N}$, ν_{N-N}, ν_{C-N}) cm^{-1}.

$[Fe(9ditz)_3](BF_4)_2$: Yield: 0.25 g (72%). $C_{33}H_{60}B_2F_8FeN_{24}$ (1022.47): calcd. C 38.77, H 5.91, N 32.88; found C 38.95, H 5.83, N 31.96. Mid-FTIR: $\tilde{\nu}$ = 3148 (ν_{C-H} of the aromatic tetrazole ring), 2933 and 2857 (ν_{C-H} of the aliphatic C–H in the butylene spacer), 1507, 1375 ($\nu_{N=N}$, ν_{C-N}), 1174, 1108 ($\nu_{C=N}$, ν_{N-N}, ν_{C-N}) cm^{-1}.

$[Fe(10ditz)_3](BF_4)_2$: Yield: 0.24 g (69%). $C_{36}H_{66}B_2F_8FeN_{24}$ (1064.55): calcd. C 40.62, H 6.25, N 31.58; found C 40.83, H 6.03, N 31.41. Mid-FTIR: $\tilde{\nu}$ = 3145 (ν_{C-H} of the aromatic tetrazole ring), 2929 and 2851 (ν_{C-H} of the aliphatic C–H in the butylene spacer), 1504, 1372 ($\nu_{N=N}$, ν_{C-N}), 1177, 1098 ($\nu_{C=N}$, ν_{N-N}, ν_{C-N}) cm^{-1}.

$[Fe(12ditz)_3](BF_4)_2$: Yield: 0.26 g (67%). $C_{42}H_{72}B_2F_8FeN_{24}$ (1148.71): calcd. C 44.15, H 6.35, N 29.42; found C 44.08, H 6.90, N 28.08. Mid-FTIR: $\tilde{\nu}$ = 3141 (ν_{C-H} of the aromatic tetrazole ring), 2917 and 2852 (ν_{C-H} of the aliphatic C–H in the butylene spacer), 1501, 1383 ($\nu_{N=N}$, ν_{C-N}), 1176, 1096 ($\nu_{C=N}$, ν_{N-N}, ν_{C-N}) cm^{-1}.

$[Fe(10ditz)_3](ClO_4)_2$: Yield: 0.20 g (55%). $C_{36}H_{66}Cl_2FeN_{24}O_8$ (1089.84): calcd. C 39.68, H 6.10, N 30.85; found C 39.03, H 5.60, N 29.23. Mid-FTIR: $\tilde{\nu}$ = 3136 (ν_{C-H} of the aromatic tetrazole ring), 2917 and 2850 (ν_{C-H} of the aliphatic C–H in the butylene spacer), 1508, 1383 ($\nu_{N=N}$, ν_{C-N}), 1178, 1088 ($\nu_{C=N}$, ν_{N-N}, ν_{C-N}) cm^{-1}.

$[Fe(12ditz)_3](ClO_4)_2$: Yield: 0.28 g (71%). $C_{42}H_{72}Cl_2FeN_{24}O_8$ (1167.94): calcd. C 43.19, H 6.21, N 28.78; found C 42.57, H 6.63, N 28.01. Mid-FTIR: $\tilde{\nu}$ = 3139 (ν_{C-H} of the aromatic tetrazole ring), 2922 and 2851 (ν_{C-H} of the aliphatic C–H in the butylene spacer), 1504, 1375 ($\nu_{N=N}$, ν_{C-N}), 1175, 1094 ($\nu_{C=N}$, ν_{N-N}, ν_{C-N}) cm^{-1}.

X-ray Powder Diffraction: The samples were gently ground and placed on flat-plate single-crystal silicon sample holders by the slurry technique with cyclohexane (Merck, p.a.) as elutriating liquid. Powder patterns were recorded with a Philips X'Pert diffractometer in Bragg–Brentano geometry using Cu-$K_{\alpha 1,2}$ radiation.

Reflectivity Measurements: Reflectivity of the samples was investigated by using a custom-built reflectivity set-up equipped with a CVI spectrometer, which allowed the collection of both the reflectivity spectra within the range of 450–900 nm at a given temperature and the following of the temperature dependence of the signal at a selected wavelength (±2.5 nm) at 5–290 K. The experiment was performed directly using a thin layer of the powdered sample without any dispersion in a matrix.[31]

Magnetic Susceptibility and Magneto-Optical Measurements: Magnetic measurements were completed with two SQUID magnetometers: (i) SQUID Cryogenix S600 magnetometer with an applied field of 1 T and (ii) MPMS-55 Quantum Design SQUID magnetometer with an operating field of 2 T within the temperature range of 2–300 K and with a cooling/heating speed of 10 $K \cdot min^{-1}$ in the settle mode at atmospheric pressure. Further measurements were made with a 9 T-PPMS-system from Quantum Design VSM operating with a field of 1 T. All magnetic measurements were performed using powder samples weighing ca. 12 mg. The data were corrected for the magnetisation of the sample holder and for diamagnetic contributions, estimated from Pascal's constants.

The photomagnetic measurements were performed using a Spectra Physics Series 2025 Kr^+ laser (λ = 532 nm) coupled by an optical fibre to the cavity of the SQUID magnetometer previously described in ref.[27] The laser light power at the sample was adjusted to 5 $mW \cdot cm^{-2}$. Bulk attenuation of light intensity was limited as much as possible by the preparation of a thin layer of compound. It is noteworthy that there was no change in the data due to sample heating upon laser irradiation. The weight of these thin layer samples (approximately 0.2 mg) was obtained by comparison of the measured thermal spin-crossover curve with another curve of a more accurately weighed sample of the same compound.

Acknowledgments

The financial support of the Austrian Science Foundation, FWF project 19335-N17, the Italian Ministero dell'Università e della Ricerca through project FIRB RBNE033KMA, and the European Community for NE "MAGMAnet" NMP3-CT-2005-515767 projects is gratefully acknowledged. Furthermore, we want to thank the European Cooperation in the Field of Science and Technology (COST) for granting A. A. a "Short Term Scientific Mission" in Bordeaux D14 and D35. Additionally, M. B. carried out research in Florence within the Marie Curie Training site LAMM (MOL-MAG-MEST-CT-2004-504204). We wish to thank the Vienna University of Technology for funding under the "Innovatives Projekt NovMat". We also wish to thank Prof. K. Mereiter (TU Vienna) for the collection of the XRPD data, Dr. M. Grunert (University of Mainz) for producing $[Fe(12ditz)_3](BF_4)_2$, Prof. G. Hilscher (TU Vienna) for SQUID measurements on the same sample, Mrs. K. Poppenberger (TU Vienna) and Mr. Y. Hasegawa (Aoyama-Gakuin University) for the SEM measurements.

[1] C. Janiak, *Dalton Trans.* **2003**, 2781–2804.
[2] Y. Garcia, V. Niel, M. C. Munoz, J. A. Real, *Spin Crossover in 1D, 2D and 3D Polymeric Fe(II) Networks* in *Topics in Current Chemistry*, vol. 233: *Spin Crossover in Transition Metal Compounds I*, Springer, Berlin, Heidelberg, **2004**.
[3] J. A. Real, A. B. Gaspar, M. C. Munoz, *Dalton Trans.* **2005**, 2062–2079.
[4] J. Schweifer, P. Weinberger, K. Mereiter, M. Boca, C. Reichl, G. Wiesinger, G. Hilscher, P. J. van Koningsbruggen, H. Kooijman, M. Grunert, W. Linert, *Inorg. Chim. Acta* **2002**, *339*, 297–306.
[5] K. Yoneda, K. Adachi, S. Hayami, Y. Maeda, M. Katada, A. Fuyuhiro, S. Kawata, S. Kaizaki, *Chem. Commun.* **2006**, 45–47.
[6] V. Ksenofontov, A. B. Gaspar, J. A. Real, P. Gütlich, *J. Chem. Phys. Lett. B* **2001**, *105*, 12266–12271.
[7] O. Roubeau, M. A. Gomez, E. Balskus, J. J. A. Kolnaar, J. J. G. Haasnoot, J. Reedijk, *New J. Chem.* **2001**, *25*, 144–150.
[8] S. Hayami, G. Juhasz, Y. Maeda, T. Yokoyama, O. Sato, *Inorg. Chem.* **2005**, *44*, 7289–7291.
[9] R. Bronisz, *Inorg. Chem.* **2005**, *44*, 4463–4465.
[10] Y. Garcia, O. Kahn, L. Rabardel, B. Chansou, L. Salmon, J. P. Tuchagues, *Inorg. Chem.* **1999**, *38*, 4663–4670.
[11] V. Niel, J. M. Martinez-Agudo, M. C. Munoz, A. B. Gaspar, J. A. Real, *Inorg. Chem.* **2001**, *40*, 3838–3839.
[12] V. Niel, A. L. Thompson, M. C. Munoz, A. Galet, A. E. Goeta, J. A. Real, *Angew. Chem. Int. Ed.* **2003**, *42*, 3760–3763.
[13] A. Galet, V. Niel, M. C. Munoz, J. A. Real, *J. Am. Chem. Soc.* **2003**, *125*, 14224–14225.
[14] G. Molnár, V. Niel, J.-A. Real, L. Dubrovinsky, A. Bousseksou, J. J. McGarvey, *J. Phys. Chem. B* **2003**, *107*, 3149–3155.
[15] V. Niel, A. L. Thompson, A. E. Goeta, C. Enachescu, A. Hauser, A. Galet, M. C. Munoz, J. A. Real, *Chem. Eur. J.* **2005**, *11*, 2047–2060.
[16] C. M. Grunert, J. Schweifer, P. Weinberger, W. Linert, K. Mereiter, G. Hilscher, M. Muller, G. Wiesinger, P. J. van Koningsbruggen, *Inorg. Chem.* **2004**, *43*, 155–165.
[17] P. J. van Koningsbruggen, Y. Garcia, H. Kooijman, A. L. Spek, J. G. Haasnoot, O. Kahn, J. Linares, E. Codjovi, F. Varret, *J. Chem. Soc., Dalton Trans.* **2001**, 466–471.
[18] B. J. Kennedy, A. C. McGrath, K. S. Murray, B. W. Skelton, A. H. White, *Inorg. Chem.* **1987**, *26*, 483–495.
[19] M. Yamada, H. Hagiwara, H. Torigoe, N. Matsumoto, M. Kojima, F. Dahan, J.-P. Tuchagues, N. Re, S. Iijima, *Chem. Eur. J.* **2006**, *12*, 4536–4549.
[20] M. Yamada, M. Ooidemizu, Y. Ikuta, S. Osa, N. Matsumoto, S. Iijima, M. Kojima, F. Dahan, J.-P. Tuchagues, *Inorg. Chem.* **2003**, *42*, 8406–8416.
[21] V. A. Money, J. Elhaik, I. R. Evans, M. A. Halcrow, J. A. K. Howard, *Dalton Trans.* **2004**, 65–69.
[22] V. Ksenofontov, H. Spiering, S. Reiman, Y. Garcia, A. B. Gaspar, N. Moliner, J. A. Real, P. Gütlich, *Chem. Phys. Lett.* **2001**, *348*, 381–386.
[23] A. Absmeier, M. Bartel, C. Carbonera, G. N. L. Jameson, P. Weinberger, A. Caneschi, K. Mereiter, J.-F. Létard, W. Linert, *Chem. Eur. J.* **2006**, *12*, 2235–2243.
[24] M. Ue, *J. Electrochem. Soc.* **1994**, *141*, 3336–3342.
[25] A. Boultif, D. Louër, *J. Appl. Crystallogr.* **1991**, *24*, 987–993.

[26] A. Hauser, *Coord. Chem. Rev.* **1991**, *111*, 275–290.
[27] a) J.-F. Létard, P. Guionneau, O. Nguyen, J. S. Costa, S. Marcén, G. Chastanet, M. Marchivie, L. Capes, *Chem. Eur. J.* **2005**, *11*, 4582–4589; b) J.-F. Létard, *J. Mater. Chem.* **2006**, *16*, 2550–2559.
[28] J.-F. Létard, L. Capes, G. Chastanet, N. Moliner, S. Létard, J.-A. Real, O. Kahn, *Chem. Phys. Lett.* **1999**, *313*, 115–120.
[29] P. L. Franke, J. G. Hasnoot, A. P. Zuur, *Inorg. Chim. Acta* **1982**, *59*, 5–9.
[30] C. M. Grunert, P. Weinberger, J. Schweifer, C. Hampel, A. F. Stassen, K. Mereiter, W. Linert, *J. Mol. Struct.* **2005**, *733*, 41–52.
[31] C. Carbonera, A. Dei, C. Sangregorio, J.-F. Létard, *Chem. Phys. Lett.* **2004**, *396*, 198–201.

Received: November 21, 2006
Published Online: May 15, 2007

